6-2015

Axial Vibrations of Brass Wind Instrument Bells and Their Acoustical Influence: Theory and Simulations

Wilfried Kausel
Institut fÄur Wiener Klangstil (Musikalische Akustik), UniversitÄat fÄur Musik und darstellende Kunst Wein , Austria

Vasileios Chatziioannou
UniversitÄat fÄur Musik und darstellende Kunst Wein, Austria

Thomas R. Moore
Department of Physics, Rollins College, TMOORE@rollins.edu

Britta R. Gorman
Rollins College

Michelle Rokni
Rollins College

Published In

Wilfried Kausel, Vasileios Chatziioannou, Thomas R. Moore, Britta R. Gorman, and Michelle Rokni. J. Acoust. Soc. Am. 137, 3149 (2015).

Axial vibrations of brass wind instrument bells and their acoustical influence: Theory and simulations

Wilfried Kausel and Vasileios Chatziioannou
Institute of Music Acoustics (Wiener Klangstil), University of Music and Performing Arts, Vienna, Austria

Thomas R. Moore,[a] Britta R. Gorman, and Michelle Rokni
Department of Physics, Rollins College, Winter Park, Florida 32789, USA

(Received 6 October 2014; revised 26 April 2015; accepted 28 April 2015)

Previous work has demonstrated that structural vibrations of brass wind instruments can audibly affect the radiated sound. Furthermore, these broadband effects are not explainable by assuming perfect coincidence of the frequency of elliptical structural modes with air column resonances. In this work a mechanism is proposed that has the potential to explain the broadband influences of structural vibrations on acoustical characteristics such as input impedance, transfer function, and radiated sound. The proposed mechanism involves the coupling of axial bell vibrations to the internal air column. The acoustical effects of such axial bell vibrations have been studied by extending an existing transmission line model to include the effects of a parasitic flow into vibrating walls, as well as distributed sound pressure sources due to periodic volume fluctuations in a duct with oscillating boundaries. The magnitude of these influences in typical trumpet bells, as well as in a complete instrument with an unbraced loop, has been studied theoretically. The model results in predictions of input impedance and acoustical transfer function differences that are approximately 1 dB for straight instruments and significantly higher when coiled tubes are involved or when very thin brass is used. © *2015 Acoustical Society of America*. [http://dx.doi.org/10.1121/1.4921270]

[JW] Pages: 3149–3162

I. INTRODUCTION

Most makers and players of brass wind instruments are convinced that wall material, wall thickness, and the positions of the bends and braces can affect both the sensation the player experiences and the sound the instrument produces when played. Because it is not obvious how these aspects of the instrument could affect the sound, there has been an ongoing debate concerning the validity of the claims. An extensive review of the history of this debate has previously been presented by Kausel *et al.*[1]

The results of experiments performed over the past decade have provided strong evidence that structural vibrations do indeed influence the radiated sound of certain brass wind instruments. Specifically, experiments on trumpets have yielded results that clearly indicate effects attributable to vibrations of the bell.[1,2] Although it is now generally accepted that structural vibrations can affect the sound produced by a brass wind instrument, to our knowledge no theory has yet been presented that can qualitatively explain and quantitatively predict the effect. However, there does seem to be a common understanding concerning which mechanisms do not contribute to the observed effects.

The vibrational modes of brass wind instrument bells that have shapes with radial nodes, referred to here as *elliptical modes*, as well as similar modes that are present in the cylindrical tubes of woodwinds and organ pipes, have been studied by Nief *et al.*[3–5] Elliptical modes are easily stimulated mechanically and during performance they can be stimulated by the vibration of the lips or by the vibrations of the air column. In either case the displacement of the metal at the antinodes of these modes can be significant. However, it can be assumed that elliptical modes are not the source of the observed timbre differences that become apparent in the sound produced by the instrument when wall vibrations are damped.[4]

The resonances associated with elliptical modes have quality factors typically exceeding 10^2 and therefore their effect is limited to a narrow band of frequencies, which is not consistent with the broad-band effects observed in several recent experiments.[1] Also, elliptical modes do not radiate efficiently due to acoustic short-circuiting and therefore the effects attributable to direct radiation are at least two orders of magnitude below those of the air column in straight tubes.[6] Similar results have been shown for these mode shapes occurring in the flaring section of trombone bells.[7] Finally, the area of an elliptical cross-section with considerable amplitude is very close to that of a perfect circle, making periodic variations of the characteristic impedance a second-order effect at best.[1]

Bending modes can also be observed in musical instruments and have been investigated by Whitehouse.[8] However, these modes can be ruled out as an explanation for timbre differences for the same reasons. The exception is that in coiled instruments they can lead to significant longitudinal bell displacements, as will be discussed later.

Mouthpiece vibrations and their interaction with the player's oscillating lips have been proposed as an explanation for timbre differences caused by structural vibrations observed during experiments with both artificial lips and

[a]Electronic mail: tmoore@rollins.edu

with real players.[2,9] Mechanical feedback of this nature may indeed have an effect on the sound, and while it is not discussed in this work it can be studied using the theoretical framework presented here. However, even without the presence of oscillating lips, consistent differences between the input impedance and acoustic transfer function (ATF) measured with and without damping of the bell of a trumpet have been observed using excitation by a loudspeaker.[1] Therefore, while it is likely that mechanical feedback to the lips of the player cannot be ignored, there are significant acoustic effects that are not associated with this mechanism.

One possible explanation for the origin of the effects due to vibrations of the walls of wind instruments was suggested by the authors in Ref. 1, where it was proposed that variations in the diameter of the pipe at the frequency of the oscillating air column couple to the internal pressure wave. In the work reported here we expand on this theory and present results demonstrating that the presence of structural resonances associated with circular modes without nodal diameters explains the broad-band characteristics of the acoustic effects attributable to wall vibrations. We refer to these structural resonances as *axial modes*. These axial modes are related to a one-dimensional (1D) wall displacement profile in the axial direction. The displacement is due to longitudinal strain oscillations or *whole body* motion. Such resonances can be shown to be broad-band in the flaring bell of a modern brass wind instrument.

In this work we present models of the King Silver Flair trumpet used in Ref. 1 and of a simplified brass wind instrument consisting of only the straight bell section of a trumpet with an attached mouthpiece. The models predict that axial resonances exist and that the axial wall motion that occurs in a relatively wide range around the first resonance frequency has the potential to affect the enclosed air column strongly enough to make an audible difference. It is possible that other axial resonances affect the air column as well.

Initially, we present a comparison between the calculated acoustical transfer function of a straight bell when it is free to vibrate and compare it to the calculated transfer function when the bell is fixed and unable to vibrate. This comparison shows that the wall vibrations can increase or decrease the amplitude of the radiated sound in a frequency range containing several air column resonances. Whether an increase or decrease occurs depends on whether the frequency of oscillation is above or below the structural resonance frequency. We also present a comparison between the calculated acoustical input impedance in the damped and undamped case. All of these results predict effects attributable to the proposed vibro-acoustic coupling.

II. STRUCTURAL VIBRATIONS

Using estimates for the local mass and stiffness of a typical trumpet bell, a 1D model was introduced in Ref. 1 that demonstrated the plausibility of the hypothesis that axisymmetric vibrations can affect the radiated sound. Below we describe a more rigorous structural model, which is global, 2D, and axisymmetric. The bore shape, wall thickness profile, Young's modulus, and Poisson's ratio are also included. This model has been implemented using an implicit finite-difference scheme of distributed point masses, with forces in both the axial and radial directions acting upon them.

External masses, springs, and dampers can be added at any point on the bore profile to represent axisymmetric approximations of braces and fittings of an experimental arrangement. These same parameters can also be used to estimate the effect of the hands, lips, and head of the player. Initial explorations of this vast parameter space have revealed a sensitivity of some acoustic parameters to these boundary conditions, which agrees with the long-held opinions of players and instrument makers.

In what follows we present the results of structural simulations of a straightened trumpet with a physical length of 137 cm and constant wall thickness of 0.4 mm. The bore list was that of a Silver Flair Trumpet in B♭. The wall thickness is changed only in the region encompassing the rim, where the mass of a typical rim wire has been added. Predictions of that model are initially compared to 2D and 3D finite element simulations performed in COMSOL, a commercial finite element analysis program that is widely used and often validated.

The model is then extended to include the interaction with the internal sound field, producing a vibro-acoustic simulation. This simulation includes the effects of wall vibrations on the acoustical characteristics such as input impedance and sound pressure transfer function.

A. Proposed vibration mechanism

Structural vibrations that have the potential to influence the radiated sound of brass wind instruments must exhibit significant vibration amplitudes over a frequency range as wide as several hundreds of Hz. Narrow band mechanical resonances, which are known to exist in brass instruments, can only affect a single note or partial and only then if the mechanical resonance frequency coincides with one of the air column resonances. Although these narrow-band resonances have been proposed as the causal mechanism for vibro-acoustic interactions in brass instruments, experiments have shown that acoustic effects, such as the differences in timbre that can be attributed to wall vibrations, occur over bandwidths much larger than those of these high-Q resonances.[10]

A second requirement is that these structural vibrations must be able to effectively modulate the cross-sectional area of the air column. Unlike pure bending modes or elliptical modes, which only very weakly translate into bore area fluctuations, mechanical vibrations responsible for the experimentally observed coupling between wall vibrations and the enclosed air must have no radial nodes.[1]

It will be shown that mechanical resonances with axisymmetric mode shapes, but with no radial nodes, meet both of these requirements. Figure 1 illustrates how such axial vibrations can translate into bore area fluctuations. The magnitude of such fluctuations is largest inside steeply flaring regions such as the bell of a trumpet. The rim is an open end of the distributed vibratory system and can be expected to be an antinode of the strongest mechanical resonances. The region near the rim is also the bore region with the steepest

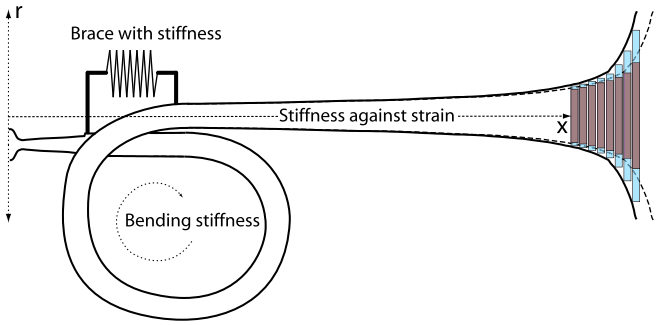

FIG. 1. (Color online) Brass wind instrument with bends and braces.

flare, and therefore it is reasonable that interaction with the air column will be most pronounced in this region. This agrees with the experimental observation that the vibrations of purely cylindrical tubing do not effectively couple with the internal air column.

To understand why axial bell vibrations translate into effective bore diameter oscillations it is convenient to use a coordinate system that is connected to the ambient air space. In this coordinate system both fluid particles of the air column as well as wall segments can have a velocity relative to the static inertial system. The diameter of an air column slice inside a flaring bore segment can change dynamically in this coordinate system, even when the wall velocity is purely axial.

The model presented here includes viscous losses, but not the viscous losses due to the additional velocity gradient inside the boundary layer that axial wall motion may create. Comparing axial wall velocities induced by the sound pressure to the corresponding air column velocities demonstrates that this loss component can be ignored in situations typically found in brass wind instruments.

One problem with using a coordinate system that is independent of the bell is that the oscillations of the bell cause the boundary of the last air-column slice to vanish periodically. This situation results in an undefined cross-sectional area of the last air column slice. This slice has a thickness corresponding to the peak-to-peak amplitude of the axial rim displacement. Fortunately there is a significant difference between the magnitude of the air velocity of the standing wave at the open mouth of the bell and the axial velocity of the rim itself. This difference is approximately an order of magnitude, therefore, this undefined but very thin final air column slice can be safely ignored.

As noted above, an appropriate coupling mechanism must explain acoustical effects which occur over a frequency range spanning several air column resonances. Axial strain oscillations can satisfy this requirement. The mechanism will be discussed qualitatively first, then the effects will be demonstrated by quantitative simulations described at the end of this section.

For any axial mode of vibration, the applied forces and inertial forces of all oscillating mass elements must be in equilibrium at all times. Therefore, according to Newton's second law, the total momentum of all oscillating mass elements must compensate the external momentum that excites the system. By accumulating all partial moments left and right of a single structural node, it can be shown that the equilibrium position of that node must shift as the frequency of oscillation changes to maintain the equilibrium of moments. This movement is due to the gradients of the axial velocity and mass distribution, both of which increase significantly in the flaring region near the rim. Therefore, there are many axial modes within a range of frequencies that contribute to a broad-band resonance. Mathematically such broad-band effects can be described as infinitely many axial modes, which are infinitesimally spaced in the frequency domain and which exhibit modal shapes with nodes that are infinitesimally shifted in their axial position. The width of this frequency range depends on the mass and stiffness distribution along the axis, which is primarily determined by the bore profile.

This mechanism results in an apparent broadband resonance that can have a considerable amplitude in a frequency range that can span multiple adjacent air column resonances. Usually there is more than one such axial broadband resonance for any given bore profile, but typically only the lowest frequency resonance is below the cutoff-frequency of a trumpet bell. We will refer to these resonances as *axial resonances*.

As will be discussed later, the vibrations described above can affect acoustical air column properties in the range of several dB even when there is only an acoustical stimulus, i.e., the sound pressure in the mouthpiece. If one assumes additional structural excitation by the vibrating lips, the effect can be increased or decreased depending on the force amplitude and the phase relationship between the lip motion and the wall vibrations.

It can be expected that axial bell vibrations of an instrument with a bend, similar to that shown in Fig. 1, will exhibit a much larger influence on the acoustical characteristics than will occur in a straight instrument without bends. This difference is attributable to the reduced axial stiffness associated with the bends.

When the mouthpiece is fixed, the strongly flaring end section of a straight bell can only move when the whole instrument is stretched or compressed against the axial stiffness of the structure, which is determined by the Young's modulus, the wall thickness and the bore profile. Treating the steeply flaring end of the bell, including the rim wire, as a mass and the remaining nearly cylindrical part as a spring, one can estimate this spring constant. Assuming a length of 40 cm, a bore diameter of 12 mm, wall thickness of 0.5 mm, and Young's modulus of 100 GPa, the spring constant can be estimated to be

$$c = E\frac{A_0}{L_0} = 100\,\mathrm{GPa} \times \pi \times 12\,\mathrm{mm} \times 0.5\,\mathrm{mm}/40\,\mathrm{cm} \approx 4.7\,\mathrm{kN/mm}.$$

The equivalent tangential spring constant of a single coil of the same tube with a coil diameter of 13 cm was determined experimentally by loading the exit cross-section tangentially with a mass and measuring the static displacement. The value was determined to be $c \approx 3.4$ N/mm. If such a coil were not stabilized by the manufacturer using a brace, shown in Fig. 1 as a stiff external spring, this low stiffness

would result in significant bell displacement amplitudes and a very low resonance frequency (<30 Hz in this case). The predicted influence of a single unbraced coil on the acoustical input impedance is discussed in Sec. IV.

B. Finite difference model

As with the model presented in Ref. 1, the model described here includes a vibrating structure with distributed mass and stiffness pairs. But here the elastic forces in both the radial and axial direction are included. They interact with the radial and axial displacement components according to Poisson's ratio and they are part of the local linear differential equations of motion. This implicit system of differential equations is discretized and then solved numerically.

Although both the axial and elliptical modes are symmetric about the axis of the bell, for ease of discussion we will use the term *axisymmetric* to refer only to mode shapes that are independent of radial angle. These mode shapes affect the circular cross section of the bell equally and with a constant phase.

As previously noted, although the narrow-band elliptical resonances are easily excited, only axial resonances can affect the internal air column efficiently enough and in a wide enough frequency range to account for the observed effects. In modeling the mechanical motion of the bell we therefore only consider motion that is independent of the radial angle. Similarly, all external and internal forces are considered to be perfectly axisymmetric.

The masses of thin cylindrical slices, or so-called hoop segments, are represented by point masses. They are connected to adjacent masses by springs representing the resistance of the wall against in-plane stress perpendicular to the circumference of the hoop segment. Circumferential elastic forces resist expansion or constriction of the bore due to an internal or external overpressure. This kind of stiffness is represented by a spring that keeps the point mass at the distance from the center of the hoop segment required by the bore radius.

Both equivalent spring constants can be calculated for the quasi-static case using Hooke's law. To obtain the effective radial spring constant, knowledge of the radial wall displacement of a single hoop segment due to a static inner air pressure is required. This relationship has been derived in Ref. 1.

The resulting equivalent spring constants derived below only depend on the Young's modulus of the wall material and some local geometric parameters. The quasi-static assumption can therefore be dropped since the air pressure is not relevant. However, discretization of the bore profile must be fine enough to allow for a sufficient number of mass points over the wave length of both the structural waves and sound waves. An axial bore resolution of 1 mm has been used for the sake of bore accuracy. This resolution also satisfies the acoustic sampling restriction.

An external mass attached to the instrument can be added to any mass point. If the corresponding radial spring stays unmodified this extra mass changes the local inertia but does not change the local stiffness. However, a modification of the local wall thickness will change both the inertia and the stiffness. The mechanics associated with the rim wire at the bell can therefore be included by adding extra mass and radial stiffness.

External springs, forces, and dampers acting on any mass point in the axial direction can also be added. As long as these external masses, springs, forces or dampers do not break the axial symmetry they can be modeled realistically. In this way braces, hands supporting the instrument, or the player's head, all of which are coupled to the instrument, can be taken into account.

We note that shear stress and bending moments have not been included in the model as yet. Usually this simplification is justified because of the small displacements leading to still smaller bending angles. But there is one case, where this assumption obviously fails. This case will be discussed in Sec. II D.

The discretization of the continuous distribution of mass and stiffness in the bell using a finite number of masses and springs for the purpose of numerical treatment is shown in Fig. 2. The equations of motion in the radial and axial directions containing all the forces acting on each mass point lead to two systems of partial differential equations that can be solved using a finite-difference frequency-domain approach.

The radial and axial displacements are related through the Poisson effect, therefore both systems of differential equations cannot be solved independently. However, radial displacements due to an expansion or constriction of the bore caused by the internal sound pressure are much smaller than the axial displacements in brass wind instruments. Therefore, we solve both systems of equations independently and take the Poisson effect of the axial displacement on the radial displacement into account in a post processing step.

Due to the axial symmetry, each lumped mass corresponds to the mass of the equivalent circular segment of brass and is given by

$$m_i = \pi\rho h(2r_i\beta + \beta^2)/\cos\theta_i, \tag{1}$$

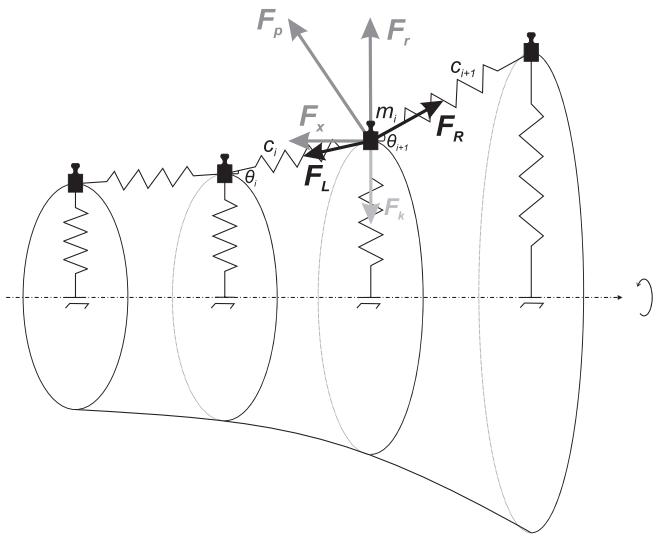

FIG. 2. Mass-spring model of the vibrating trumpet wall (Ref. 11). The symbols are defined in the text.

where m_i is the mass of segment i, r_i its internal radius, β its thickness, and h the axial distance between the masses. The distance h is taken to be the axial grid spacing, which is chosen to be 2 mm. The length of each segment at rest is given by $L_i = h/\cos\theta_i$, where θ is the flare angle. The force due to the internal pressure p applied on the walls of each segment is given by

$$F_p(i) = 2\pi r_i p_i h/\cos\theta_i, \tag{2}$$

and is always perpendicular to the wall. Therefore, the radial and axial components of the force due to internal pressure can be calculated as

$$F_r(i) = 2\pi r_i p_i h, \tag{3}$$

$$F_x(i) = -2\pi r_i p_i h \tan\theta_i. \tag{4}$$

The spring constants of the springs between the masses, calculated using Hooke's law, are given by

$$c_i = \frac{2\pi r_i \beta E}{h/\cos\theta_i} = 2\pi r_i \beta E \cos\theta_i/h. \tag{5}$$

The radial spring constants can be calculated using the definition of a spring constant as $k_i = F_r(i)/s_i$, where $s_i = p_i r_i^2/(E\beta\cos^3\theta_i)$ is the amplitude of the radial wall displacement and $F_r(i)$ the radial pressure force.[1] Therefore, the radial spring constants are given by

$$k_i = 2\pi\beta E h\cos^3\theta_i/r_i. \tag{6}$$

At the rim of the bell the brass is folded around a wire, referred to as the rim wire. This constitutes an extra mass that can affect the structural resonances. Including this in the model requires increasing the mass of the final segment and modifying the stiffness of the last radial spring.

The model also includes the Poisson effect, which describes the stretch in one dimension caused by a strain in another dimension. As noted above, the displacements in the axial direction are much greater than those in the radial direction, therefore, only processes in which the radial displacement is affected by the axial displacement are considered. This simplification allows one to solve for the axial displacement first, neglecting any effects due to radial displacement. The accompanying radial displacement can then be calculated using Poisson's ratio.

One equation of motion for each direction is necessary. For the axial displacement

$$\begin{aligned} m_i\ddot{x} &= F_{Rx}(i) + F_{Lx}(i) + F_x(i) \\ &= F_R(i)\cos\theta_{i+1} + F_L(i)\cos\theta_i + F_x(i) \\ &= c_{i+1}\Delta L_{i+1}\cos\theta_{i+1} - c_i\Delta L_i\cos\theta_i + F_x(i), \end{aligned} \tag{7}$$

where x is the axial displacement, $F_{Rx}(i)$ and $F_{Lx}(i)$ are the axial components of the spring forces to the right and left of mass m_i, and ΔL_i is the deformation of the spring with stiffness c_i. Substituting a single-frequency solution of the form $x_i = X_i e^{j\omega t}$ and simplifying yields

$$c_i X_{i-1} + (m_i\omega^2 - c_i - c_{i+1})X_i + c_{i+1}X_{i+1} + F_x(i) = 0, \tag{8}$$

where X_i corresponds to the complex amplitude of the axial displacement of mass m_i and ω is the angular frequency. Similarly, for the radial displacement, the corresponding equation of motion is

$$c_i Y_{i-1} + (m_i\omega^2 - c_i - c_{i+1} - k_i)Y_i + c_{i+1}Y_{i+1} + F_r(i) = 0. \tag{9}$$

The total displacement in the radial direction can be calculated by adding the contribution from the axial displacement,

$$Y_{\text{tot}} = Y_i + Y_{Xi} = Y_i - r_i\nu\frac{X_{i+1} - X_{i-1}}{2h}, \tag{10}$$

where ν is Poisson's ratio. Solving Eqs. (8), (9), and (10) for each frequency makes it possible to determine the displacement at any point on the wall. Results of this model are compared to corresponding finite-element simulations in Sec. II D.

C. Finite-element analysis

The model introduced in Sec. II B can be used to predict many of the experimental effects reported previously,[1,2,12] as well as predicting new phenomena that can be tested experimentally. However, it is useful to compare these predictions with those of a fully 3D finite-element (FE) model. In so doing it is possible to understand some of the limitations of the mass-spring model as well as determine how necessary a fully 3D calculation is to predict the observed effects.

The implementation of a finite element model of the straight trumpet bell with the attached mouthpiece described in Sec. II A was performed using COMSOL. The thickness and bore profile were provided by the manufacturer.

The simplification of using a straight bell eliminates several degrees of freedom due to the simple symmetry. It also assists the manufacturer in maintaining precise dimensions and material properties. Both of these should improve the agreement between modeling and experimental results compared to the previous attempt reported in Ref. 13, where modeling results were compared with measurements made on a complete trumpet.

Due to the axial symmetry, finite element modeling in 2D should be sufficient to capture all of the behavior that can be compared to the mass-spring model. However, a full 3D frequency domain analysis has also been performed to show the elliptical modes of vibration. These elliptical modes can serve as a cross-check of the structural parameters because it is easy to verify those frequencies experimentally. Additionally, while it is known that these vibrational modes do not significantly affect the radiated far-field sound of brasses unless they are tuned to an air column resonance,[3,5] these modes can be used to validate the material constants used in the simulations.

One of the most difficult parts of the bell to model is the rim. This is because the rim is made by folding the metal

back over the rim wire, which is then soldered in place. Rather than attempting to determine the appropriate physical parameters, the frequencies of the elliptical resonances of the bell were measured using decorrelated electronic speckle pattern interferometry[14] and the radius and mass of the rim enclosing the rim wire was chosen so that the frequency of the (2,1) elliptical mode, corresponding to two nodal diameters and one nodal circle, matched the measured frequency.

Using a constant bell thickness and standard values for brass density (8400 kg/m^3), Young's modulus (110 GPa), and Poisson's ratio ($\nu = 0.35$), the frequencies of many elliptical modes were predicted to be close to the frequencies measured using electronic speckle pattern interferometry. Any discrepancies can be explained by the imperfect circular cross-section of the bell.

Variations in the thickness of the walls is especially important because they are assumed to be constant in the model. The thickness of the straight bells, while reported as being constant by the manufacturer, exhibited variations of up to 17% along the circumference of the bell and up to 12% along the axis when measured using a Magna Mika 8500® thickness gauge.

These thickness variations should be expected given the manner in which the bells of brass instruments are manufactured, and they will undoubtedly shift resonance frequencies and change operating deflection shapes. Along with the solder seam, which adds a line with different material properties to the contour of the bell, these variations can break the axial symmetry. Therefore, mode splitting of axial vibration modes is expected to occur in bells manufactured in the traditional manner.

D. Results and comparison of different methods

Although the 3D FE model provides a more precise model of the bell under investigation than the mass-spring model introduced in Sec. II B, the two models should compare well in situations where the essential physics is captured by the more simple model. Therefore, it is useful to compare the results of the two models.

The 3D finite element model of the trumpet bell was simulated as being stimulated at the mouthpiece plane by a sinusoidal force acting in the axial direction with an amplitude of 1N. This amplitude is on the order of what is expected to be present due to lip motion during actual performance. A small perturbation with 1 mN orthogonal to the main stimulus force was included to break the symmetry of the model. This perturbation ensured that elliptical modes could also be excited.

The predicted displacement of the rim of the bell is plotted in Fig. 3, along with the prediction of a corresponding axisymmetric (2D) finite element simulation. Clearly the assumption of symmetry along the axis only results in the failure to predict some narrow-band resonances at a limited number of frequencies, each of which corresponds to resonances having elliptic or bending mode shapes.

There is one resonance corresponding to an axisymmetric mode, which we will term the *rim mode*, that is predicted by both of the finite element simulations, but not predicted when

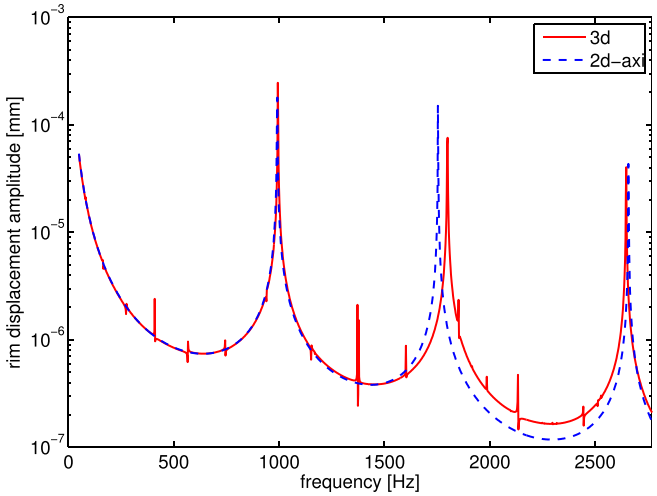

FIG. 3. (Color online) Rim displacement amplitude as a function of frequency stimulated by a force applied at the mouthpiece calculated using a 2D axisymmetric (dashed) and a 3D (solid) finite element model.

using the finite difference scheme described in Sec. II B. This deflection shape is characterized by an antinode at the rim with a nodal circle just a few centimeters away from the rim. It significantly deforms the structure near the end of the bell and its frequency is determined primarily by the bending stiffness rather than the strain resistance of the brass sheet. This deflection shape can be described as a rotational motion of all rim segments around the circular nodal line. Since this motion involves rotational forces and rotational moments of inertia, which are not included in the finite difference model, the model cannot predict such resonances.

Although the finite difference model cannot predict this kind of motion, which is shown in Fig. 4, this motion at the extremity of the bell will not radiate efficiently due to the dipole nature with dimensions small compared to the wavelength of excitation. Therefore, we do not expect a significant acoustic effect. It is, however, possible that this resonance can coincide with and de-tune the second longitudinal resonance.

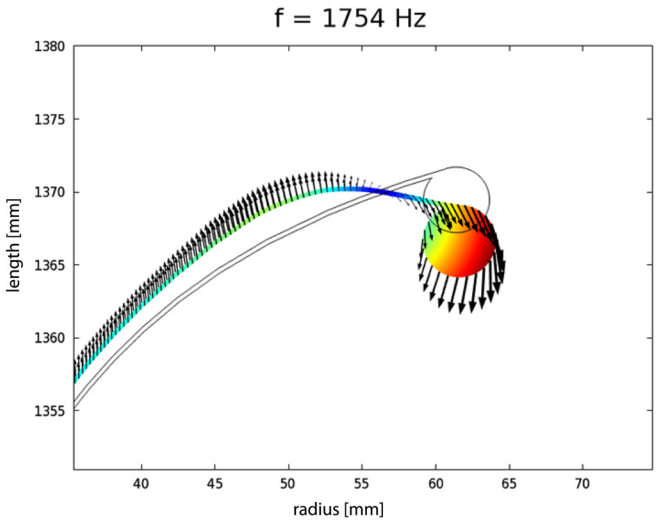

FIG. 4. (Color online) Second axial resonance deformation, i.e., the *rim-mode,* scaled by a factor of 3000 to show the existence of a node very close to the rim, calculated using a 2D finite element model.

TABLE I. First and second axial resonance frequencies for a trumpet with and without a rim, as calculated using a 2D or 3D finite element model (FEM) and the presented mass-spring model (MS).

	Rim-wire			No rim-wire		
	FEM 3D	FEM 2D	MS	FEM 3D	FEM 2D	MS
f_1	994	991	1018	1133	1134	1125
f_{rim}	1799	1754				
f_2	2648	2658	2413	2519	2546	2543

In this case it will be difficult to predict the frequencies of this resonance accurately with the simple finite-difference model.

Table I shows predictions of all three models for the first two longitudinal axial resonances and for the rim mode described above. Note that the frequency of the second axial resonance calculated by the FE models varies significantly from that calculated by the mass-spring model. Presumably this is because the second resonance has a node very close to the rim and is therefore affected by rotational motion. Removing the rim-wire from the simulation detunes this resonance significantly, with the result being that the predictions of all three models agree. These results are shown in the second column of Table I. Animations of the first axial and (2,1) elliptic mode shapes are shown in Figs. 5 and 6.

As a final test of the simple finite difference model, the vibrational response to the distributed force stimulus of a realistic acoustic sound pressure profile has been calculated and compared to a corresponding COMSOL result. The sound pressure profile of the enclosed air column, calculated using BIAS,[15] was applied as a boundary load to the interior of the bell walls in the mass-spring model and in a corresponding axisymmetric 2D finite element model.

A comparison of the axial and radial displacement amplitudes along the bore profile of the King Silver Flair trumpet modeled without bends predicted by the two models is depicted in Fig. 7, where the solid lines represents the results of the mass-spring model and the dashed lines represent the results of the 2D FE model. The sinusoidal pressure in the mouthpiece was 250 Pa. The excitation frequencies of

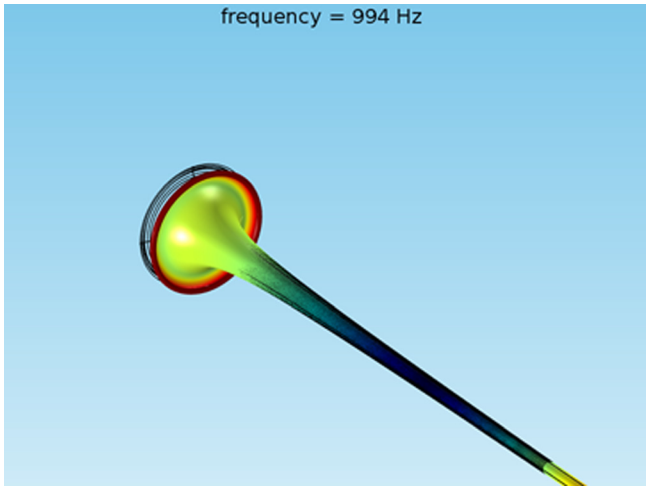

FIG. 5. (Color online) Animation of the motion of the first axial resonance. The predicted frequency is 994 Hz (see Ref. 27).

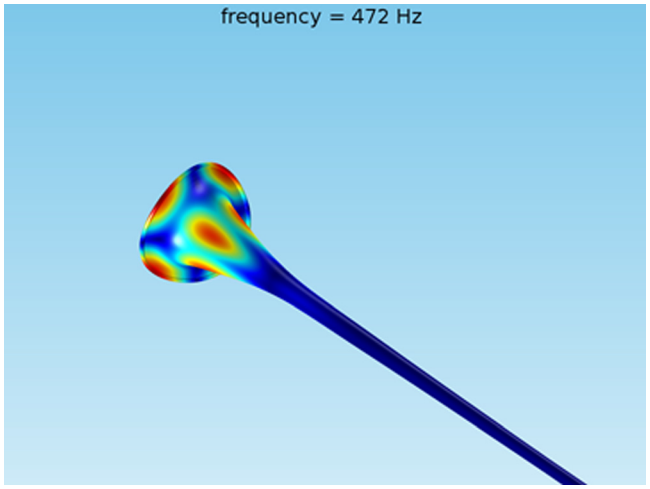

FIG. 6. (Color online) Animation of the (2,1) elliptical mode shape. The predicted frequency is 472 Hz (see Ref. 27).

486 and 1069 Hz correspond to the fourth and ninth peak of the input impedance.

Clearly the mass-spring model can capture much of the essential physics of the situation. The fact that the rotational degree of freedom of the rim is not captured by the mass-spring model explains the difference between the two methods in predicting the displacement in close proximity of the rim. Since the instrument is excited at the frequency of an air-column resonance, the frequency difference between the excitation and the second structural resonance, which is a rim mode in one of the cases, depends on the model used. This results in different predictions for the displacement amplitudes, but as noted previously, it is unlikely that this resonance affects the radiated sound of the instrument.

Figure 8 shows how operating deflection shapes smoothly vary with frequency, a property of the proposed axial vibration mechanism which was discussed qualitatively above. These curves were obtained using the mass-spring model of a standard trumpet bell without bends, connected to a mouthpiece with a total physical length of 73 cm and discretized into bore slices of 1 mm. The graph shows the magnitudes of the axial vibration amplitudes plotted as a function of the axial distance from the mouthpiece plane, when stimulated at the mouthpiece end by an axial, sinusoidally oscillating mechanical force of 1 N and an in-phase mouthpiece pressure of 250 Pa. The amplitude and phase relationship have been chosen arbitrarily. The mechanical stimulus represents a conservative estimate for a possible contact force applied by a player's lips.

The model parameters have been chosen to match an existing standard trumpet bell made from brass by an instrument maker. The bell was straight, without the usual bend. The simulation parameters were: Young's modulus $E = 100$ GPa, density $\rho = 8440$ kg/m^3, Poisson's ratio $\nu = 0.35$, and damping factor $\tan\delta = 0.05$. These results clearly indicate that the proposed vibration mechanism can result in significant motion in the bell region over a relatively wide frequency band.

The wall thickness of 0.55 mm is slightly larger than that found in most trumpets, but still typical for some instruments. Since it was expected that wall vibration effects will

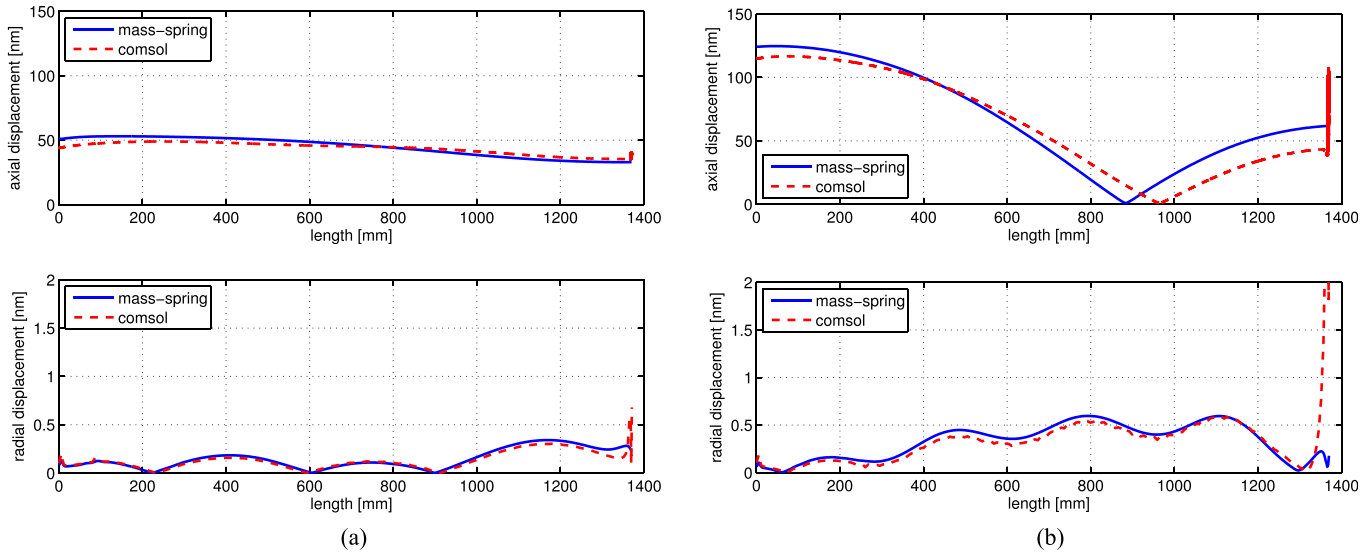

FIG. 7. (Color online) Axial (top) and radial (bottom) wall displacement amplitude as a function of position, caused by a 250 Pa sinusoidal mouthpiece pressure at (a) 486 Hz and (b) 1069 Hz, calculated using the mass-spring model (solid) and a 2D finite element model (dashed).

become stronger when wall thickness decreases, a thicker wall material helps to estimate a lower bound for the magnitude of the effect. We expect the effects to exceed these predictions in real instruments.

The unusually high inner damping factor of 0.05 was determined experimentally by connecting the bell to a shaker and sweeping through the expected first axial resonance. The amplitude of the axial rim displacement relative to that of the driving point was measured at several different points, averaged in order to eliminate the effects of elliptic modes, and plotted against the theoretical curve. The inner damping factor was then used as a fitting parameter and the value was chosen to produce the best agreement between theory and experiment.

This inner damping factor is usually written as $\tan(\delta)$ and it refers to the tangent of the argument of a complex Young's modulus. Its value is normally assumed to be on the order of 0.001 for brass, which is fifty times smaller than the value determined experimentally as described above. The reason for this significant deviation has yet to be determined, but two possible reasons are discussed below.

First, inner damping of metals is not well addressed in the literature and to our knowledge there is no report that posits the dependence of $\tan(\delta)$ on common metal treatments such as molding, bending and annealing. It is worth noting that the people who manufacture brass musical instruments appear to be universally convinced of the importance of these processes in determining the final sound.

It is also possible that the uneven wall thickness profiles around the perimeter and along the axis, combined with the general deviation from a perfect circular symmetry that is inevitable in the manufacturing process, may have an overall effect which can be predicted by adding a factor into the imaginary part of the complex Young's modulus. Given the importance of mechanical resonances and their bandwidth to the final sound of brass instruments indicated by the work

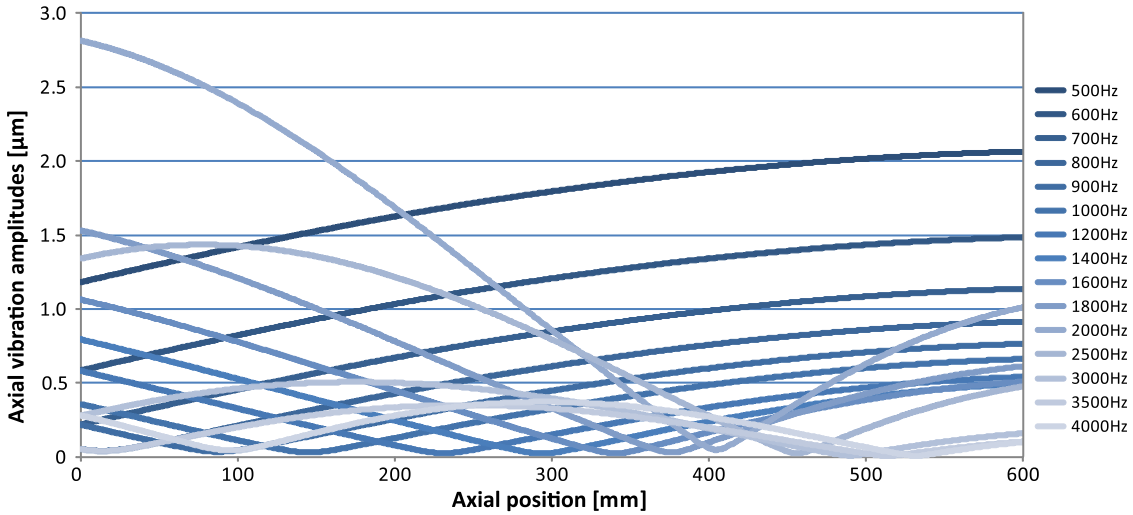

FIG. 8. (Color online) Axial vibration amplitude profiles at various frequencies of a straight trumpet bell connected to a mouthpiece when stimulated acoustically and mechanically at the mouthpiece end.

reported here, it is important that the origin of this discrepancy be determined in the near future.

Finally, it should be noted that other critical parameters, such as Young's modulus and the density may vary with composition and treatment of the wall material. Reconstructing the actual values by a parameter matching optimization routine using measured structural characteristics, as has been done in this work, may be the only practical way to accurately determine all of the important parameters.

III. VIBRO-ACOUSTIC INTERACTION

Wave propagation inside a wind instrument has been extensively studied and successfully modeled in the past.[16–18] In these cases, the walls of the instrument are usually considered to be perfectly rigid, however, this is not the case when brass wind instruments are actually used in performance. Apart from the possibility of mechanical feedback to the player's lips, there is a coupling between the vibrating walls and the air column inside the instrument that can affect its input impedance.[3,4,19–22]

The structural model described above can be used to predict wall vibrations induced by the sound pressure inside the instrument as well as by oscillating forces applied to any part of the instrument. This allows one to study the effect of wall material, mechanical damping, mass and stiffness distribution, and oscillating forces exerted by the vibrating lips on the mouthpiece rim.

In this section we address the question of how to incorporate the structural model described above into an algorithm that can calculate the input impedance and ATF of wind instruments, taking into account the effects of wall vibrations stimulated by the interior acoustic field as well as by external oscillating forces.[23] A vibro-acoustic interaction model was proposed by the authors in Ref. 1, but this model was derived for the isothermal case. Here we address the adiabatic case, which is more applicable to the conditions found in wind instruments.

As noted above and illustrated in Fig. 1, axial vibrations translate into radial air column boundary oscillations inside flaring sections of the bore. Additionally, there is a smaller contribution due to the Poisson effect. These radial boundary vibrations affect the enclosed air column through two separate mechanisms. First, they create a parasitic acoustic volume flow $\widehat{\Delta u}$ into the vibrating wall as discussed in Sec. III B. Second, they modulate the volume of all bore segments, which periodically changes the local air density and therefore the local air pressure by an amount of $\widehat{\Delta p}$, which is addressed in Sec. III C. All quantities marked by a caret (such as $\widehat{A}$) are complex, frequency-dependent amplitudes; they are the coefficients of the usually omitted term $e^{\mathrm{j}\omega t}$ and represent harmonically oscillating values with a constant magnitude and phase.

Both contributions can be treated as distributed sound flow and pressure sources with wavelets that propagate and interfere with each other along the bore to produce an accumulated effect at the mouthpiece plane. Each local point source $\widehat{\Delta p}(x)$ transmits a wavelet towards the input plane being modified by its distance-dependent transfer function $\widehat{A}(x)$ to generate an accumulated extra sound pressure $\widehat{\Delta p_0}$ at the mouthpiece plane,

$$\widehat{\Delta p_0} = \int_0^L \widehat{\Delta p}(x)\widehat{A}(x)dx. \tag{11}$$

The distributed volume flow is accumulated in a similar way, back-propagated to the entrance plane by the flow related transfer function $\widehat{B}(x)$. In a discretized bore profile consisting of purely cylindrical or conical segments the transfer functions $\widehat{A}(x)$ and $\widehat{B}(x)$ for sound pressure and flow can be obtained from the product of the transfer matrices of all segments,[15,16] which back-propagate p and u from the plane at axial position x to the entry plane at $x=0$.

As we are integrating both contributions over the axial length of the instrument, care must be taken so as to not integrate the volume flow u twice. When calculating the flow u, as shown below, it is the contribution lost into the walls of a short cylindrical segment of length h. If we wish to integrate this contribution we first must divide it by the length h to obtain a flow contribution per unit length. This can then be integrated

$$\widehat{\Delta u_0} = \int_0^L \frac{\widehat{\Delta u}(x)}{h}\widehat{B}(x)dx. \tag{12}$$

A. Modified transmission line model

The starting point of the vibro-acoustic interaction model is the 1D plane-wave transmission-line model as implemented in Ref. 23 and reviewed in Ref. 15. It allows the calculation of input impedance and pressure transfer function of acoustic ducts such as brass or woodwind instruments when their bore profile and radiation conditions are known.

The model provides complex, frequency-dependent transmission matrices

$$\widehat{T} = \begin{pmatrix} \widehat{T}_a & \widehat{T}_b \\ \widehat{T}_c & \widehat{T}_d \end{pmatrix} \tag{13}$$

for each cylindrical or conical slice of the bore profile. The variable pair pressure $\widehat{p}$ and volume flow $\widehat{u}$ are then transmitted from the right side of the element to the left side according to

$$\begin{aligned} \widehat{p}_1 &= \widehat{T}_a\widehat{p}_2 + \widehat{T}_b\widehat{u}_2, \\ \widehat{u}_1 &= \widehat{T}_c\widehat{p}_2 + \widehat{T}_d\widehat{u}_2. \end{aligned} \tag{14}$$

Assuming unity sound pressure at the open mouth of the bell, a volume flow of $\widehat{u}_{\mathrm{Bell}} = 1/\widehat{Z}_{\mathrm{rad}}$ is enforced by the radiation impedance $\widehat{Z}_{\mathrm{rad}}$. Back propagating $\widehat{p}$ and $\widehat{u}$ using the transmission matrices of all bore elements, an input pressure $\widehat{p}_0$ and volume flow $\widehat{u}_0$ at the mouthpiece end of the bore can be obtained. From this result the input impedance $\widehat{Z}_{\mathrm{in}} = \widehat{p}_0/\widehat{u}_0$ and pressure transfer function $\widehat{T}_p = \widehat{p}_{\mathrm{rad}}/\widehat{p}_0$ can be derived.

Taking the vibrating walls into account can be achieved by modifying all inner $\widehat{p}_i$, $\widehat{u}_i$ pairs according to $\widehat{p}_i^* = \widehat{p}_i + \widehat{\Delta p}_i$,

with $\widehat{u}_i^* = \widehat{u}_i + \widehat{\Delta u}_i$, with $\widehat{\Delta p}_i$ and $\widehat{\Delta u}_i$ being the complex sound pressure and volume flow amplitudes lost due to the oscillating wall. This addition results in

$$\begin{aligned}\widehat{p}_1 &= \widehat{T}_a(\widehat{p}_2 + \widehat{\Delta p}_2) + \widehat{T}_b(\widehat{u}_2 + \widehat{\Delta u}_2),\\ \widehat{u}_1 &= \widehat{T}_c(\widehat{p}_2 + \widehat{\Delta p}_2) + \widehat{T}_d(\widehat{u}_2 + \widehat{\Delta u}_2).\end{aligned} \tag{15}$$

Alternatively the wall vibration effect can be taken into account by correcting the conventional transfer matrix elements $\widehat{T}_a$ and $\widehat{T}_c$ by multiplying them by the factor $(\widehat{p}_2 + \widehat{\Delta p}_2)/\widehat{p}_2$. Likewise, the elements $\widehat{T}_b$ and $\widehat{T}_d$ can be adjusted using the factor $(\widehat{u}_2 + \widehat{\Delta u}_2)/\widehat{u}_2$.

B. Flow into the vibrating wall

An effective velocity $\widehat{v}(x) = \widehat{d}(x)\omega$ can be calculated with the effective wall displacement amplitude

$$\widehat{d}(x) = \widehat{d}_{\text{radial}}(x) - \widehat{d}_{\text{axial}}(x)\tan(\phi(x)), \tag{16}$$

where ϕ is the flare angle and $\widehat{d}$ is the radial and axial components of the local wall displacement amplitudes. Note that a positive axial displacement in conjunction with a positive flare angle actually reduces the effective boundary diameter for a given air column slice, which explains the negative sign in Eq. (16).

The volume flow $\widehat{\Delta u}$ into the vibrating wall of a short hoop segment with length h is given by

$$\widehat{\Delta u}(x) = \widehat{v}(x)2r(x)\pi h, \tag{17}$$

where $r(x)$ is the local bore radius. This contribution has a positive instantaneous value when the momentary wall velocity v is also positive, which is the case when the hoop segment expands. A positive instantaneous in-flow into the left boundary of an element can therefore be either compensated by a positive instantaneous out-flow out of the right boundary of that element or by some positive parasitic flow into the walls. If the total flow is not balanced the pressure will change $(d\widehat{p}/dt = \widehat{u}_{\text{Left}} - \widehat{u}_{\text{Right}} - \widehat{\Delta u})$.

The simplifying assumption made here is that only mass continuity (in-flow equals total out-flow) is taken into account while the balance of momentum and energy is neglected. This is justified because the mean thermal velocity of air, which is given by $v_{\text{rms}} = \sqrt{3k_{\text{B}}T/m}$ in m/s, where k_{B} is Boltzmann's constant, T is temperature in K, and m is the mass of an air molecule in kg, dominates all velocities related to flow that may result in other pressure related forces.

C. Thermodynamic pressure modulation

During an adiabatic process the ideal gas equation is given by

$$p(t)V^{\gamma}(t) = n(t)RT, \tag{18}$$

where the pressure $p(t)$, volume $V(t)$, and number of moles $n(t)$ all vary with time. T is the equilibrium temperature, γ the heat capacity ratio, and R the universal gas constant. In the presence of the vibrating walls the volume oscillations with an amplitude $\widehat{V}$ must be included in the pressure variation.

Following Ref. 1, but considering adiabatic conditions, the effective time varying pressure deviation (p_+) can be obtained from the equilibrium pressure p_{eq} by means of a Taylor series expansion. Neglecting second order terms this expansion becomes

$$\widehat{p} + e^{\mathrm{j}\omega t} = \widehat{p}e^{\mathrm{j}\omega t} - \gamma\frac{p_{\text{eq}}}{V_{\text{eq}}}\widehat{V}e^{\mathrm{j}\omega t}, \tag{19}$$

where V_{eq} is the equilibrium volume of the air column and $\widehat{p}$ the complex amplitude of the oscillating air column pressure without the presence of wall vibrations. The phase difference between this internal pressure and the wall oscillations is reflected in the phase difference between the complex amplitudes $\widehat{p}$ and $\widehat{V}$. Hence the extra pressure amplitude due to wall oscillations is given by

$$-\widehat{\Delta p} = \gamma\frac{p_{\text{eq}}}{V_{\text{eq}}}\widehat{V} = \gamma\frac{p_{\text{eq}}}{\pi r^2 h}(2\pi r h\widehat{s}) = \frac{2\gamma p_{\text{eq}}}{r}\widehat{s}, \tag{20}$$

where $\widehat{s}$ the complex amplitude of the effective radial displacement of the air column boundary and we have suppressed the position dependence for notational clarity. The negative sign indicates that an in-phase radial wall displacement actually reduces the local sound pressure amplitude.

IV. RESULTS AND DISCUSSION

In all of the vibro-acoustic simulations reported here we have used parameters and bore shapes derived from two similar straight trumpet bells with wall thicknesses of 0.5 mm and 0.55 mm manufactured by *Musik Spiri*. Measurements of the thicker bell were used to produce the curves shown in Fig. 8, and the material properties stated above were applied to both bells, unless otherwise stated.

A typical simulation result for the 0.55 mm bell without a mouthpiece is shown in Fig. 9. The mouthpiece end was rigidly fixed by adding an extremely heavy mass at that point. The top plot depicts the two ATF curves representing the ratio of the sound pressure amplitude in the bell plane to that in the entrance plane. One calculation takes wall vibrations into account while the other one represents the case of a completely rigid wall. The differences between the ATF corresponding to the rigid case and that corresponding to the case where the bell is allowed to vibrate freely are small but noticeable. The ratio of the two ATFs is shown in the bottom plot using a dB-scale.

The results shown in Fig. 9 indicate that the differences in the ATF below approximately 800 Hz are always positive while those above that cross-over frequency are always negative. The magnitudes of these differences reach their maximum in close proximity to the frequency that corresponds to the phase transition at the first axial resonance. In this example this structural resonance does not coincide with any of the air resonances, but occurs between the second and third acoustic resonance. Differences due to wall vibrations are

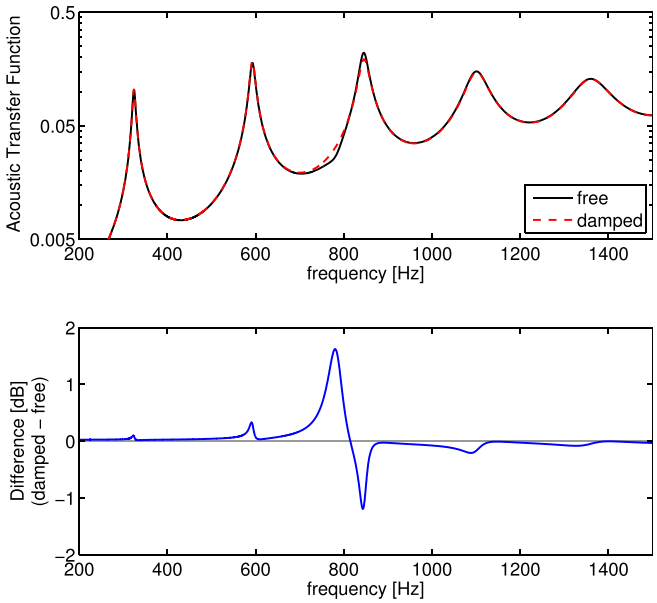

FIG. 9. (Color online) Simulated ATF of a straight bell without a mouthpiece from the entrance plane to bell plane as a function of frequency, for the case of a free vibrating bell (solid) and completely damped bell (dashed). The bottom plot shows the difference in dB.

small but noticeable over a range of frequencies corresponding to approximately one octave.

Another kind of influence is shown in Fig. 10, where the calculated difference in the input impedance that results from bell vibrations is plotted. In this case the 0.5 mm bell has been chosen with a standard mouthpiece attached to it. The mouthpiece was loaded with an extra mass of 2 kg to represent the weight of a horn driver, which may be required when performing an experiment. To help orient the reader, the frequencies of the maxima of the underlying input impedance curve have been shown in the plot as vertical lines.

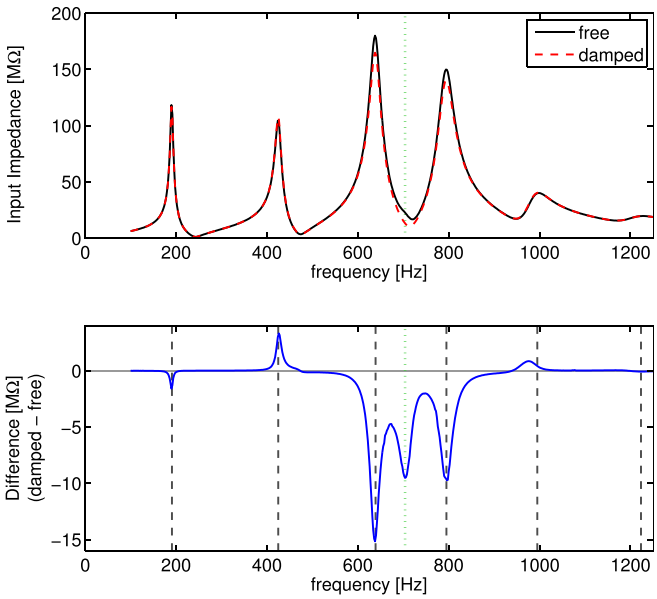

FIG. 10. (Color online) Input impedance of the free and damped bell (top) and the difference between the two curves (bottom) calculated numerically. The dashed lines indicate the locations of the impedance peaks and the dotted line indicates the frequency of the axial structural resonance of the bell.

This plot is the result of two vibro-acoustic finite element simulations run in COMSOL, again one with a rigid bell and one with a bell free to vibrate.

In the finite-element model used to produce the curves in Fig. 10 a thin boundary layer next to the wall, where the flow is retarded due to frictional losses,[13] was discretized using a boundary layer mesh with each element's thickness being approximately 1 μm. The air domain was discretized using a frequency-dependent mesh-size, ensuring that at least ten elements per wavelength are present. A detail of the mesh is shown in Fig. 11, where the sound pressure level is also plotted for the first air resonance of the straight bell. Finally, a perfectly matched layer was simulated as surrounding the semi-spherical radiation space to enforce anechoic conditions. A baffle was also simulated to avoid feedback to the input pressure, as is often the case when performing experiments.[1,2,12,24]

The relative size of the differences at the third and fourth air resonance in Fig. 10, where the input impedance is approximately 150 MΩ, is again on the order of one decibel. However, in this case the effect of the cross-over frequency between the third and the fourth air resonance is different. We can observe an alternating influence below the structural resonance (minus-plus-minus) and an alternating influence above it (minus-plus-minus). Around the structural resonance this alternation is toggled, which leads to two adjacent peaks with the same negative difference surrounding the cross-over frequency corresponding to the first axial resonance.

These observations lead to the question of why there are two, and possibly more, fundamentally different kinds of influences on acoustical characteristics which are obviously due to the same structural resonance. To answer this question we must consider all possible excitation mechanisms and their effects on the acoustic field inside the instrument.

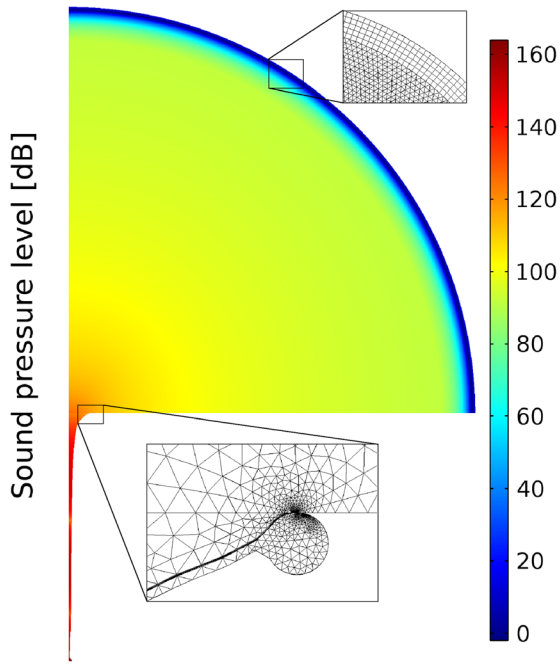

FIG. 11. (Color online) Sound pressure level for a free vibrating bell, showing details of the underlying finite-element mesh.

A brass wind instrument bell is an acoustic duct with one end closed and the other end open. This means that the sound pressure magnitude profile must have a maximum at the mouthpiece and a minimum near the open end of the bell. At the lowest resonance frequency the mouthpiece pressure and the pressure inside the bell are in phase. At the next resonance frequency a second pressure minimum finds its place inside the instrument. This inverts the phase relationship and causes the pressure at the mouthpiece and bell to be out of phase. At still higher resonances each new pressure minimum inside the instrument again alternates the phase of the sound pressure in the steeply flaring part of the bell relative to the sound pressure present in the mouthpiece.

A longitudinal structural stimulus at the mouthpiece will cause an in-phase displacement of the bell if the frequency is low. Near DC there will be whole-body motion and all parts of the bell will move synchronously and at the same velocity. At higher frequencies periodic stress will cause axial strain which adds length oscillations. Below a structural resonance the bell displacement will still be almost in phase with the mouthpiece stimulus. At a structural resonance, however, the phase changes and above the resonance frequency the axial bell motion will be out of phase with the motion at the mouthpiece.

The internal sound field is mainly affected in the flaring bell region, but there are two possibilities to stimulate structural vibrations by the interior sound pressure. In the mouthpiece the sound pressures may be up to a factor of 10^3 higher than in the bell region and the area that the pressure can act on is approximately 60 times smaller than the comparable area in the bell region. Therefore, the dominating structural stimulus can be situated either in the mouthpiece or in the bell region, or it can be a combination of the two depending on the frequency-dependent parameters related to the bore profile and boundary conditions.

If the dominating structural stimulus mechanism is in the bell region there will be an acoustical effect exhibiting the same phase for all air resonances below structural stimulus, with the opposite phase for air resonances above it. The structural resonance frequency will be the cross-over frequency for any effect of wall vibrations on any acoustic characteristic. In the simulation shown in Fig. 9 this behavior has been enforced by applying a large mass to the entrance plane, thus fixing it in place.

In the case where the mouthpiece is attached to the bell but is free to vibrate it is possible that the structural stimulus of the sound pressure inside the mouthpiece cup dominates the effects attributable to the bell motion. This may occur if the mouthpiece diameter is large and the axial mechanical admittance of the mouthpiece is much higher than that of the bell. In this case, the behavior shown in Fig. 10 is expected because the alternating phase of the effect is related to the alternating phase of the sound pressure in the bell compared to the sound pressure in the mouthpiece, which is synchronously exciting both the acoustical and mechanical systems.

For the time being, only straight axisymmetric bells can be simulated using the mass-spring model presented here. However, an application to a complete instrument with a single loop similar to that shown in Fig. 1 is shown in Fig. 12. Using a coiled brass tube with a coil diameter of 14 cm, a bore diameter of 10.8 mm, and a wall thickness of 0.4 mm, the effective stiffness of a spring linking the lead pipe and the straight part of the bell in axial direction was determined experimentally to be 3400 N/m. A spring with this spring constant was added to the model by adjusting the stiffness of the cylindrical tube section between 19 and 90 cm. This has been accomplished by reducing the wall thickness in this region to 1 μm and compensating for the removed mass of the wall. A crosscheck of the equivalent spring constant yields $c = 100\,\text{GPa} \times \pi \times 10.8\,\text{mm} \times 1\,\mu\text{m}/71\,\text{cm} \approx 4.6\,\text{kN/mm}$ which is close to what was measured. The first axial resonance of this arrangement was determined to be approximately 30 Hz.

Figure 12 shows that the acoustic influence of the vibrating bell potentially can make a more significant difference in this configuration. In this case the vibrating bell acts to damp all resonances above the structural resonance and it is likely that an instrument maker will try to shunt that spring using a brace with much higher stiffness. The behavior is consistent with Fig. 9 because a vibrating bell which transmits better above the structural resonance does

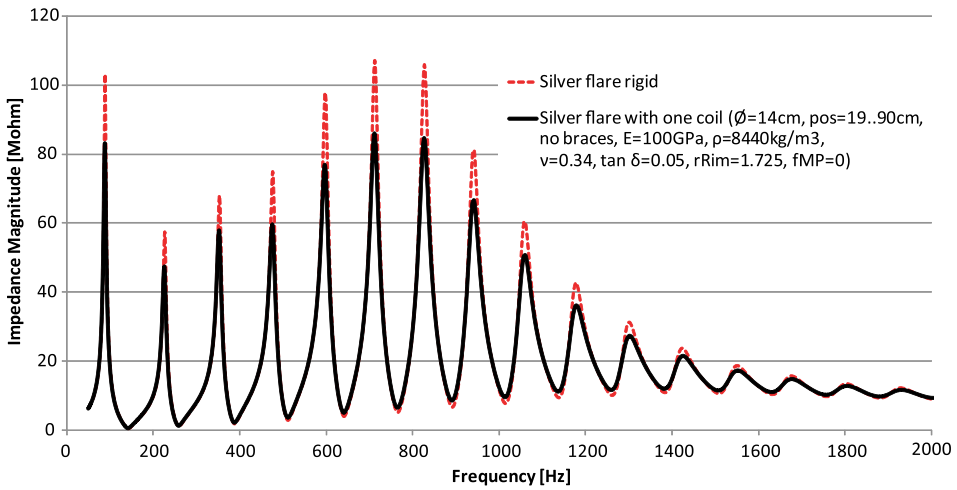

FIG. 12. (Color online) Input impedance of a trumpet with one coil for the case of a bell free to vibrate (solid) and when the vibrations are completely damped (dashed).

not reflect well in the same frequency range, which lowers the input impedance.

V. CONCLUSIONS

The model discussed here predicts that axial resonances have a measurable effect on the sound of brass wind instruments. It is likely that these effects explain the sensitivity to construction details that are commonly claimed by musicians and makers of musical instruments. As presented, the model can predict most aspects of the essential structural behavior of axisymmetric brass wind instrument bells and their effect on the acoustical characteristics. This model can predict the acoustical and mechanical transfer functions as well as the acoustical input impedance in the presence of vibrations induced by external sources or by the pressure fluctuations of the internal air column.

The model can include external structural excitations, such as those of the player's vibrating lips, and allows one to include external masses, springs, and damping at any part of the bore profile to reflect how the instrument is held, clamped, or stimulated. Subtle details like a non-constant wall thickness profile along the axis, a mouthpiece mass profile, or a unique rim wire construction can also be specified. Exploring this vast parameter space is beyond the scope of this work, but as a preliminary result it can be stated that most of these external influences, such as mechanical stimulation by player's lips, braces that stiffen loops and bends, different rim wire constructions, and extra masses attached to the mouthpiece can have an even stronger influence on acoustical parameters than what is shown in the simulations reported here.

We expect that this model will aid in understanding the effects of the different kinds of influences that wall vibrations have on acoustic characteristics of brass wind instrument bells. To facilitate these investigations, the model has been implemented in the Brasswind Instrument Analysis System (BIAS)[25] and can be downloaded from Ref. 26. Within this implementation of the simulation it is possible to specify arbitrary bore and wall thickness profiles as well as user-specified boundary conditions and material constants.

Using such hybrid models, which combine measured mechanical transfer functions and physical structural models of some axisymmetric parts, the effect of wall vibrations on the sound of real instruments can be predicted. This can even include structural excitation by the player's lips. Once the vibration state of the mouthpiece can be predicted it will be possible to study its effect on the lip oscillator and therefore on the oscillation threshold and response of an instrument.

Predictions of this model have yet to be completely validated by experiments. Of particular importance is the prediction that the acoustical effects of wall vibrations should be inverted at the frequencies of axial resonances due to the change in phase between the oscillating air column and the oscillating wall that occurs at these frequencies. Preliminary experimental results indicate that this does indeed occur.[12]

ACKNOWLEDGMENTS

The authors thank Werner Spiri and the *Musik Spiri* company for manufacturing the straight trumpet bells. The portion of this work performed at Rollins College was supported by Grant No. PHY-1303251 from the National Science Foundation.

[1]W. Kausel, D. W. Zietlow, and T. R. Moore, "Influence of wall vibrations on the sound of brass wind instruments," J. Acoust. Soc. Am. **128**, 3161–3174 (2010).

[2]T. R. Moore, E. T. Shirley, I. E. Codrey, and A. E. Daniels, "The effects of bell vibrations on the sound of the modern trumpet," Acta Acust. Acust. **91**, 578–589 (2005).

[3]G. Nief, "Comportement vibroacoustique des conduits: Modelisation, mesure et application aux instruments de musique a vent" ("Vibroacoustic behavior in ducts: Modalisation, measurement and application to musical wind instruments"), Ph.D. thesis, Laboratoire d'acoustique de l'universite du Maine, Le Mans, France (2008).

[4]G. Nief, F. Gautier, J.-P. Dalmont, and J. Gilbert, "Influence of wall vibrations on the behavior of a simplified wind instrument," J. Acoust. Soc. Am. **124**, 1320–1331 (2008).

[5]G. Nief, F. Gautier, J.-P. Dalmont, and J. Gilbert, "External sound radiation of vibrating trombone bells," in *Proceedings of Acoustics'08*, SFA, Paris, France (2008), pp. 2447–2451.

[6]J. Backus and T. C. Hundley, "Wall vibrations in flue organ pipes and their effect on tone," J. Acoust. Soc. Am. **39**, 936–945 (1966).

[7]A. Morrison and P. Hoekje, "Internal sound field of vibrating trombone bell," J. Acoust. Soc. Am. **101**, 3056 (1997).

[8]J. Whitehouse, "A study of the wall vibrations excited during the playing of lip-reed instruments," Ph.D. thesis, Open University, Milton Keynes, United Kingdom (2003).

[9]P. Hoekje, "Vibrations in brass instrument bodies: A review," J. Acoust. Soc. Am. **128**, 2419 (2010).

[10]W. Kausel, "It's all in the bore! – Is that true? Aren't there other influences on wind instrument sound and response?," J. Acoust. Soc. Am. **121**, 3177 (2007).

[11]W. Kausel, V. Chatziioannou, and T. Moore, "More on the structural mechanics of brass wind instrument bells," in *Proceedings of Forum Acusticum 2011*, European Acoustics Association, Aalborg, Denmark (2011), pp. 527–532.

[12]B. Gorman, M. Rokni, T. Moore, W. Kausel, and V. Chatziioannou, "Bell vibrations and how they affect the sound of the modern trumpet," in *Proceedings of the International Symposium on Musical Acoustics 2014*, Institut Technologique Europen des Mtiers de la Musique, Le Mans, France (2014), pp. 215–218.

[13]V. Chatziioannou and W. Kausel, "Modelling the wall vibrations of brass wind instruments," in *Proceedings of the COMSOL Conference* 2011, Stuttgart, Germany (2011).

[14]T. R. Moore and J. J. Skubal, "Time-averaged electronic speckle pattern interferometry in the presence of ambient motion. Part I: Theory and experiments," Appl. Opt. **47**, 4640–4648 (2008).

[15]W. Kausel, "Bore reconstruction of tubular ducts from acoustic input impedance curve," IEEE Trans. Instrum. Meas. **53**, 1097–1105 (2004).

[16]D. Keefe, "Acoustical wave propagation in cylindrical ducts: Transmission line parameter approximations for isothermal and nonisothermal boundary conditions," J. Acoust. Soc. Am. **75**, 58–62 (1984).

[17]N. H. Fletcher and T. D. Rossing, *The Physics of Musical Instruments*, 2nd ed. (Addison-Wesley, New York, 1990), pp. 190–232.

[18]D. Keefe, "Woodwind air column models," J. Acoust. Soc. Am. **88**, 35–51 (1990).

[19]R. Picó, J. Gilbert, and F. Gautier, "The wall vibration effect in wind instruments: Effect induced by defaults of circularity," in *Proceedings of the International Symposium on Musical Acoustics, ISMA 2007*, Univerisitat Politecnica de Catalunyia, Institut d'Estudis Catalans, Barcelona, Spain (2007).

[20]G. Nief, F. Gautier, J.-P. Dalmont, and J. Gilbert, "Influence of wall vibrations of cylindrical musical pipes on acoustic input impedances and on sound produced," in *Proceedings of the International Symposium on Musical Acoustics, ISMA 2007*, Univerisitat Politecnica de Catalunyia, Institut d'Estudis Catalans, Barcelona, Spain (2007).

[21]V. Chatziioannou, W. Kausel, and T. Moore, "The effect of wall vibrations on the air column inside trumpet bells," in *Proceedings of the Acoustics 2012 Nantes Conference*, Nantes, France (2012), pp. 2243–2248.
[22]W. Kausel, V. Chatziioannou, B. Gorman, M. Rokni, and T. Moore, "Vibro acoustic modeling of wall vibrations of a trumpet bell," in *Proceedings of the International Symposium on Music Acoustics, ISMA 2014*, Le Mans, France (2014), pp. 89–93.
[23]A. Braden, D. Chadefaux, V. Chatziioannou, S. Siddiq, C. Geyer, and W. Kausel, "Acoustic Research Tool (ART)," http://sourceforge.net/projects/artool (Last viewed 05/18/2015).
[24]F. Gautier and N. Tahani, "Vibroacoustic behaviour of a simplified musical wind instrument," J. Sound Vib. **213**, 107–125 (1998).
[25]G. Widholm, H. Pichler, and T. Ossmann, "BIAS—a computer aided test system for brass instruments," Audio Engineering Society preprint No. 2834 (1989), pp. 1–8.
[26]G. Widholm, W. Kausel, and A. Mayer, "Brasswind Instrument Analysis System (BIAS)," http://bias.at (Last viewed 05/18/2015).
[27]See supplemental material at http://dx.doi.org/10.1121/1.4921270 for animation of the motion of the first axial resonance (predicted frequency is 994 Hz) and of the (2,1) elliptical mode shape (predicted frequency is 472 Hz).